

AN5006: Probing the aggregation rate of Tau protein with automated DLS and SLS

Abhisek Mukherjee, Ph.D.¹, Jason Lin, Ph.D.², Sophia Kenrick, Ph.D.²

¹ University of Texas Health Science Center at Houston; ² Wyatt Technology Corporation

Summary

In this work, batch dynamic and static light scattering in the DynaPro[®] Plate Reader are used to investigate the aggregation of tau proteins, which have been observed to form neurofibrillary tangles in patients suffering from neurodegenerative diseases. Light scattering provides quick and easy-to-use methods to 1) screen starting materials, 2) measure aggregation rate on the nanometer scale, and 3) probe size distributions for greater insights into aggregation mechanism.

Introduction

The main function of tau is the stabilization of microtubules. Self-aggregation of tau proteins is a characteristic of a number of neurodegenerative diseases, such as Alzheimer's disease and Parkinson's disease^{1,2}. Understanding the aggregation pathway can help develop better screening tools, treatment options, and possible prevention of these diseases.

There are a number of techniques to measure tau aggregation, including sedimentation assays, qualitative and quantitative electron microscopy, and intrinsic and extrinsic fluorescence³. However, these techniques can suffer from disadvantages, such as the inability to detect or quantify small proteins (tau monomer ~45-65 kDa), the requirement of an external dye or marker (extrinsic fluorescence), and the lack of tryptophan residues in many tau constructs (intrinsic fluorescence).

In this work, the aggregation rate of tau proteins was measured with dynamic and static light scattering using the DynaPro Plate Reader. Light scattering measurements overcome many of the challenges of traditional aggregation assays for tau⁴. The molecules can be measured in solution without the addition of an external probe and without requiring any specific amino acids. In

addition, the high throughput format of the DynaPro Plate Reader enables measurements to be made *in situ* over a variety of conditions and without disturbing the samples.

Materials and Methods

Solutions of soluble tau proteins and seed aggregates were provided by Professor Claudio Soto at The University of Texas Health Science Center at Houston.

A DynaPro Plate Reader was used to analyze all samples. Solutions of tau proteins were created with and without seeds, filtered to 0.02 μm and dispensed into a 96 well plate (Corning). For each solution, 100 μL of sample was dispensed in duplicate into the well plate. Microwell plate-sealing tape (Nunc) was applied to prevent evaporation, and the plate was immediately inserted into the DynaPro Plate Reader, which was preset to 37 °C. Data collection, including images of each well, and light scattering data analysis were performed with DYNAMICS[®] software.

Quality control data (Results and Discussion: Section 1) were measured immediately after inserting the well plate into the DynaPro Plate Reader. The aggregation rate (Section 2) was assessed by scanning all wells every thirty minutes over the course of fourteen hours. Size distribution data (Section 3) were monitored throughout.

Results and Discussion

Section 1. Quality control of starting materials

In order to assess the initial stages of aggregation, it is important to ensure starting materials are pure and free of contaminating particles. In this case, the tau "monomer" appeared to be a uniform solution of species with radius ~10 nm. This value is much larger than expected for a globular protein or linear polymer with the

same molar mass as the tau monomer (65 kDa). This large observed size suggests that oligomeric “pre-aggregates” are present in the solution, rather than pure monomers, though for convenience we will continue to refer to this solution as “monomers.”

The autocorrelation functions (ACF) for tau solutions with and without seeds are shown in Figure 1. Both autocorrelation functions display a single, smooth decay, representative of a predominantly monomodal sample. The data were fit to a cumulant model, yielding $R_h = 11.9 \pm 0.2$ nm for the “monomer” and $R_h = 17.4 \pm 0.8$ nm for the seeded samples. The fit residuals shown in Figure 1 are small and random, which supports the use of a cumulants analysis and implies the solution is dominated by a single diffusion coefficient (hydrodynamic radius) with some standard deviation (polydispersity).

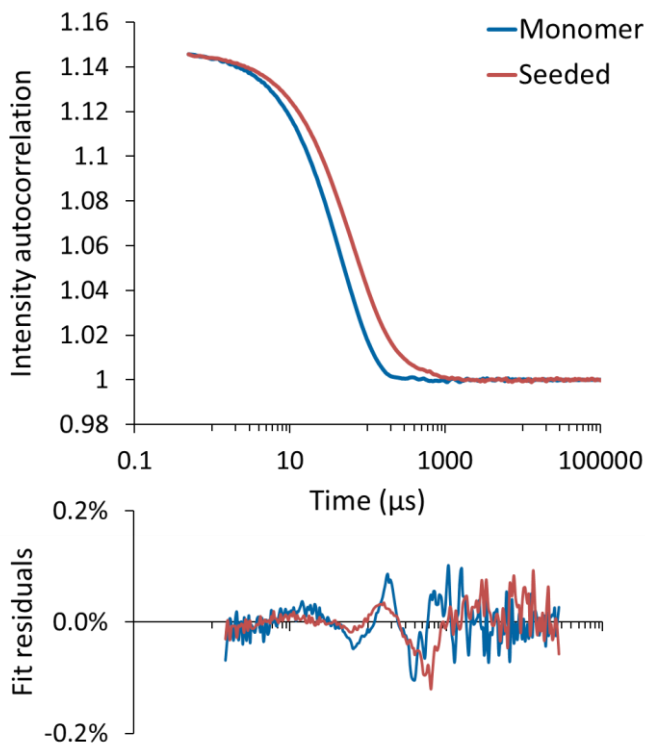


Figure 1: Autocorrelation function for tau monomer (blue) and seeded with aggregates (red). The bottom panel shows the fit residual between the measured ACF and cumulants fit.

Even within the first five minutes of incubation at 37 °C, there is an appreciable increase in the average hydrodynamic size for the solution containing seeds (17.4 nm compared to 11.9 nm), which is visible in the ACF (Figure 1). In addition, the polydispersity of the seeded sample is significantly larger than that of the “monomer” sample. Both of these data sets support the hypothesis that the tau monomer has already begun to aggregate in the presence of these seed particles. It is important to note that, although the aggregate seeds measured >500 nm, they were added to the solution at such a low concentration that they did not contribute appreciably to the scattering intensity and were not considered a separate species by regularization analysis (see Section 3, “Size distribution of tau and aggregates”).

Section 2. Measuring tau aggregation rate

Oligomeric tau species in the “monomer” solution appear stable over multiple hours at 37 °C. The hydrodynamic radius and light scattering intensity for these molecules was constant as a function of time, suggesting no further aggregation was taking place (Figure 2, blue diamonds). In fact, both measures remained constant for over 14 hours.

A change in size required the introduction of a small amount of aggregate seeds. The seeds caused immediate and steady aggregation, resulting in an increase in both hydrodynamic radius and total scattering intensity (Figure 2, red squares). Since the normalized intensity is proportional to the weight-average molar mass of the solution, we can conclude the change in size is due to an increase in molar mass, rather than a conformational change.

Aggregation rate data were fit to a polynomial in DYNAMICS software (Figure 2, dashed lines). The “monomer” data were fit to a zero-order polynomial, yielding an average hydrodynamic radius of 12.0 nm and average light scattering intensity of 3.1×10^4 kCnt/s. For the seeded tau solution, the initial aggregation rate was determined by fitting the first hour of data to a straight line. The seeded tau grew at an initial rate of 13.7 nm/h, and the intensity increased at a rate of 4.5×10^4 (kCnt/s)/h.

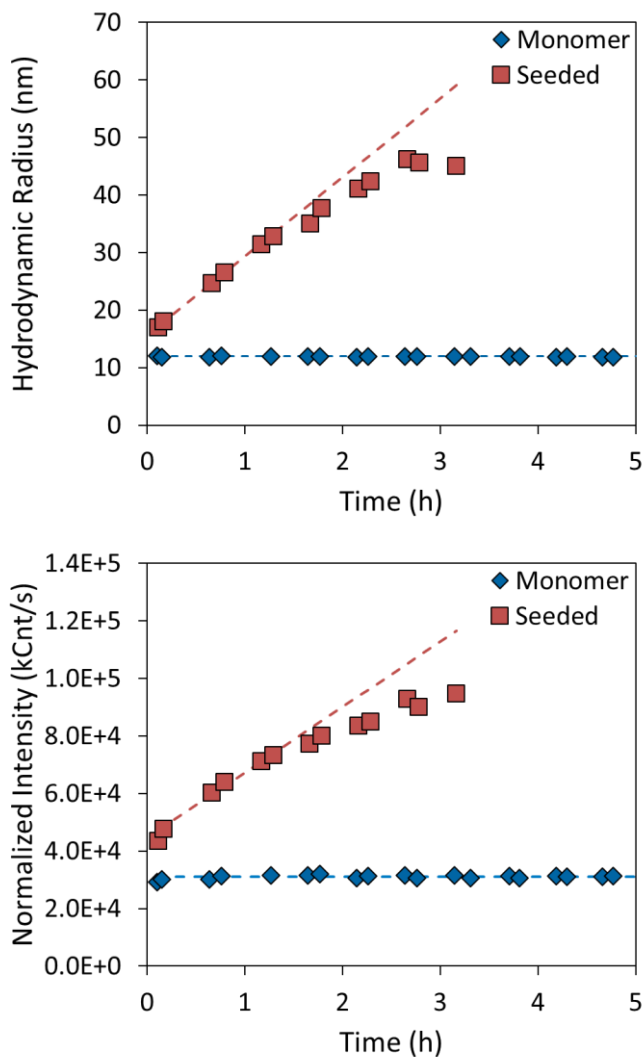


Figure 2: Measurement of tau aggregation rate in the presence (red squares) or absence (blue diamonds) of aggregate seeds. The top panel shows the increase in hydrodynamic radius as a function of time, and the bottom panel shows the normalized intensity.

Section 3. Size distribution of tau and aggregates

The data in Figure 2 were generated by fitting the ACF to a cumulants model to provide an average particle radius. This type of analysis is useful for observing trends over time and calculating aggregation rate, but it does not reveal any information about the particle size distribution. In the DYNAMICS software, the ACF can also be fitted with a regularization model to generate size distribution plots. Figure 3 shows the size distribution plots for the tau solutions as a function of time. At an early timepoint, both solutions are predominantly composed of a single size species with radius ~ 10 -20 nm. This agrees with Figure 1 which showed that both solutions fit well to the cumulants model at early timepoints.

Over the first three hours, the size distribution of the “monomer” tau solution does not exhibit any significant change. In contrast, the tau solution with aggregate seeds starts off as a monomodal size distribution and evolves into a bimodal distribution within one hour. Over the course of three hours, the population with radius ~ 10 nm decreases while an aggregate population with radius ~ 200 nm increases. This observation coupled with the aggregation rate in Figure 2 may provide greater insights into the aggregation mechanism.

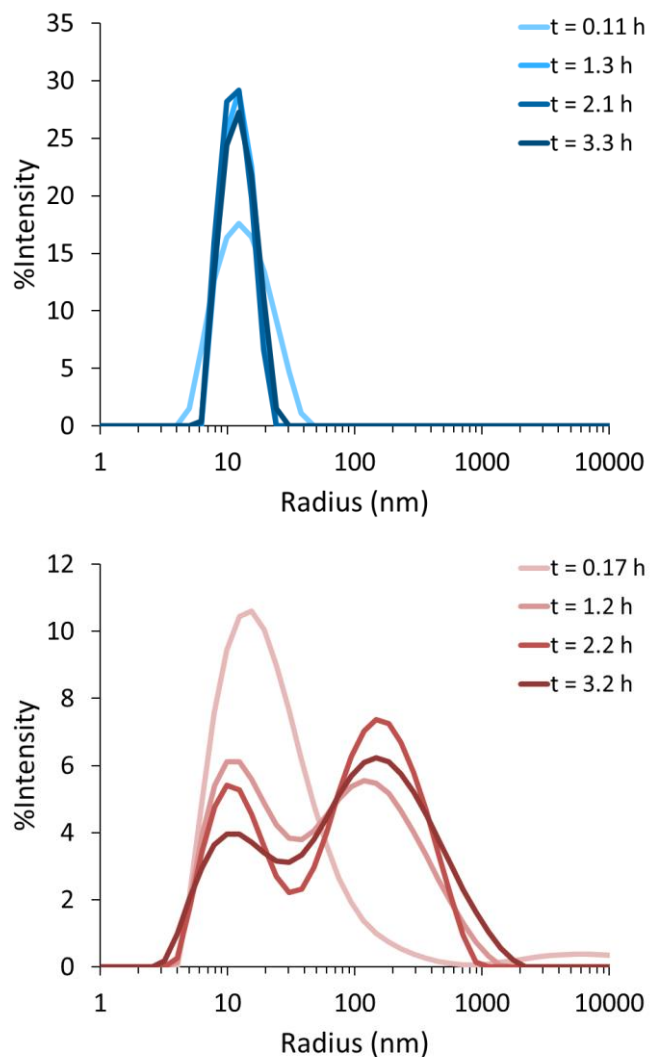


Figure 3: Distribution of particle sizes for tau protein solution (top) and aggregate-seeded tau solution (bottom) as a function of incubation time at 37 °C. Histograms for initial measurements are colored lightest, and measurements after ~ 3 hours of incubation are colored the darkest.

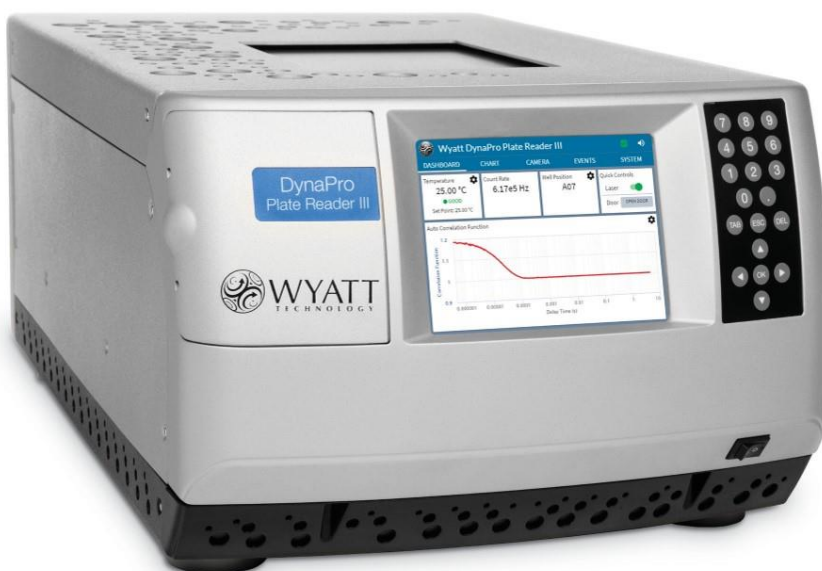
Conclusions

Dynamic light scattering, employing the DynaPro Plate Reader to monitor multiple samples and conditions in parallel, provided unique insights into the aggregation of proteins associated with neurodegenerative diseases. In this case, the tau “monomer” solution was found to contain oligomers with hydrodynamic radius ~ 10 nm. These pre-aggregates were stable at 37 °C for over 14 hours.

The growth of tau oligomers into larger aggregates occurred only after the addition of aggregate seeds. Tau aggregation appeared to occur immediately upon addition of the seeds even without agitation. Not only was the aggregation rate determined by light scattering, but changes in size distribution were also quantified, which may lead to a better understanding of the aggregation mechanism.

References

1. Soto, C. In Vivo Spreading of Tau Pathology. *Neuron* **73**, 621–623 (2012).
2. Arrasate, M., Pérez, M., Armas-Portela, R. & Ávila, J. Polymerization of tau peptides into fibrillar structures. The effect of FTDP-17 mutations. *FEBS Lett.* **446**, 199–202 (1999).
3. Luo, J., He, R. & Li, W. The fluorescent characterization of the polymerized microtubule-associated protein Tau. *Int. J. Biol. Macromol.* **27**, 263–268 (2000).
4. Zhu, H.-L. *et al.* Quantitative characterization of heparin binding to Tau protein: implication for inducer-mediated Tau filament formation. *J. Biol. Chem.* **285**, 3592–3599 (2010).



© Wyatt Technology Corporation. All rights reserved. No part of this publication may be reproduced, stored in a retrieval system, or transmitted, in any form by any means, electronic, mechanical, photocopying, recording, or otherwise, without the prior written permission of Wyatt Technology Corporation.

One or more of Wyatt Technology Corporation's trademarks or service marks may appear in this publication. For a list of Wyatt Technology Corporation's trademarks and service marks, please see <https://www.wyatt.com/about/trademarks>.